量子ビームでさぐるソフトマターの物性

Shear-induced structural phase transition

瀬戸秀紀

CROSS

High Energy Accelerator Research Organization

Effect of interlamellar interactions on shear induced multilamellar vesicle formation

Y. Kawabata, S. Kugizaki (Tokyo Metropolitan U.)

R. Bradbury, M. Nagao (NIST and Indiana U.)

K. Weigandt (NIST)

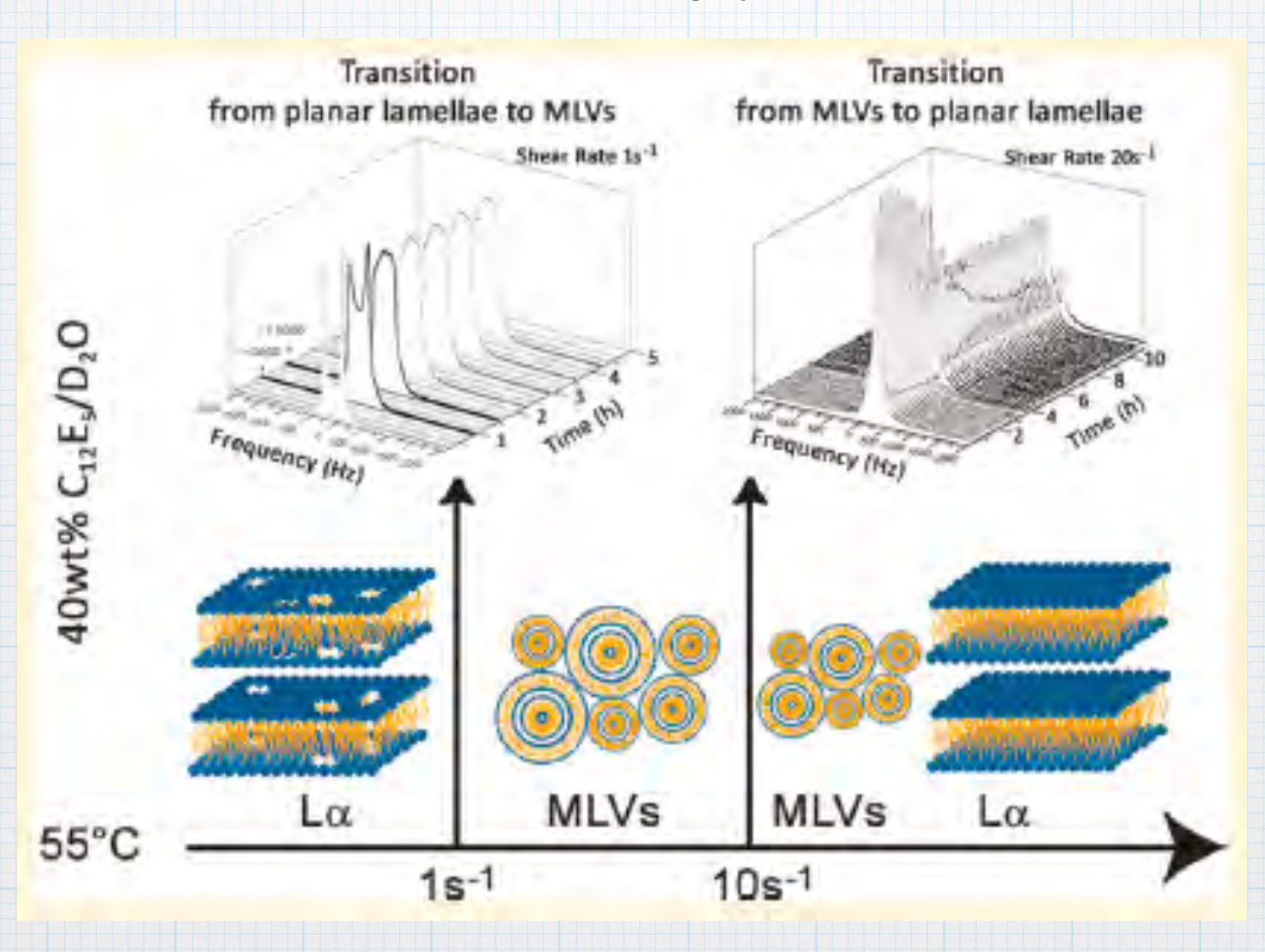
Y. B. Melnichenko (ORNL)

K. Sadakane (Doshisha U.)

N. L. Yamada, H. Endo, H. Seto (KEK)

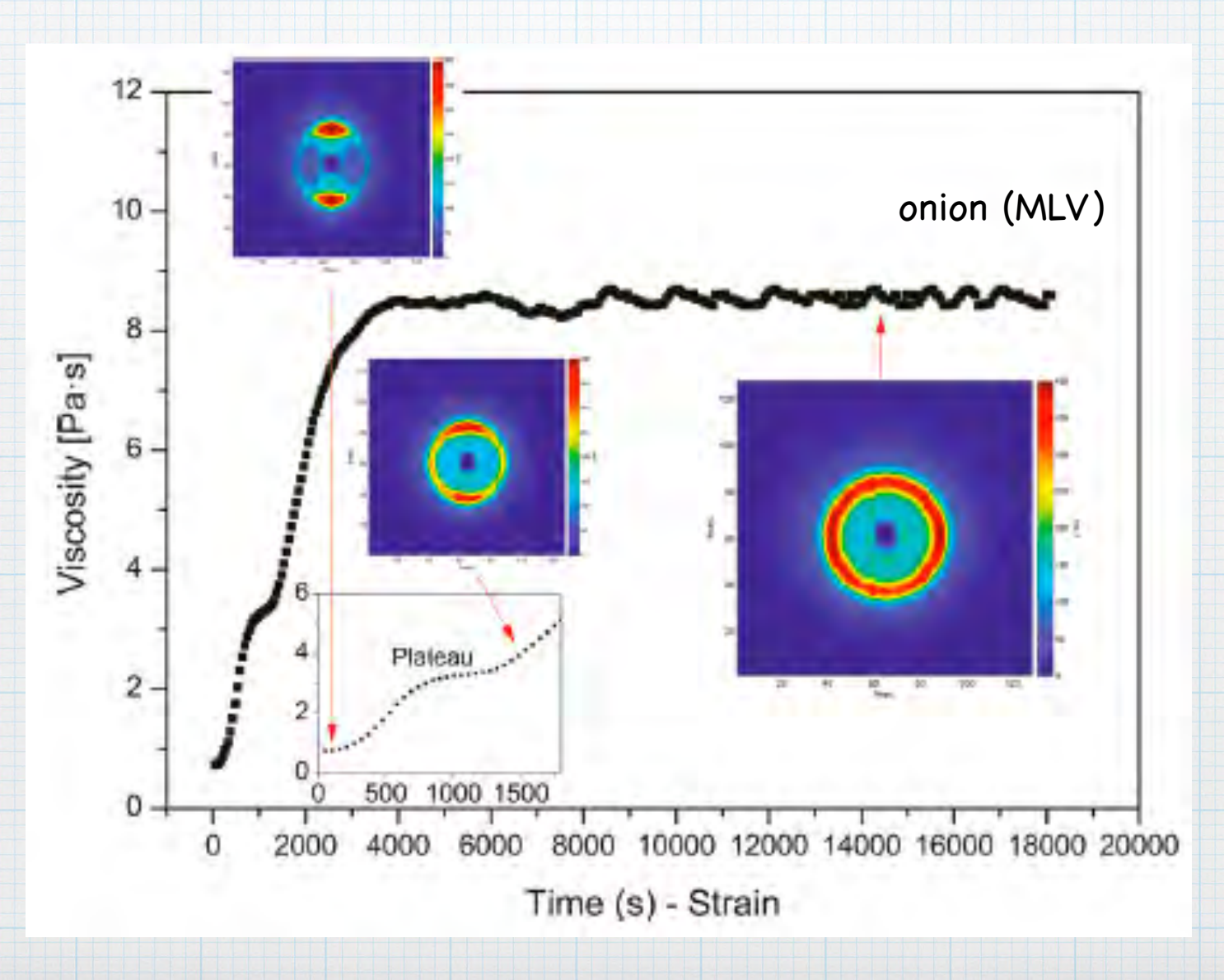
Y. Kawabata et al., J. Chem. Phys., 147, 035905 (2017).

water / C₁₂E₅

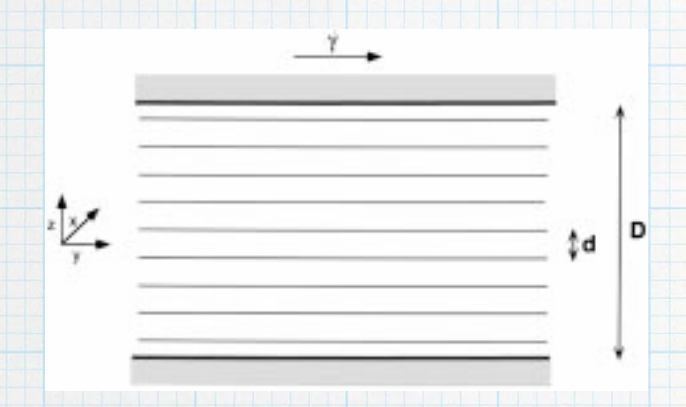


Shear-thickening is observed

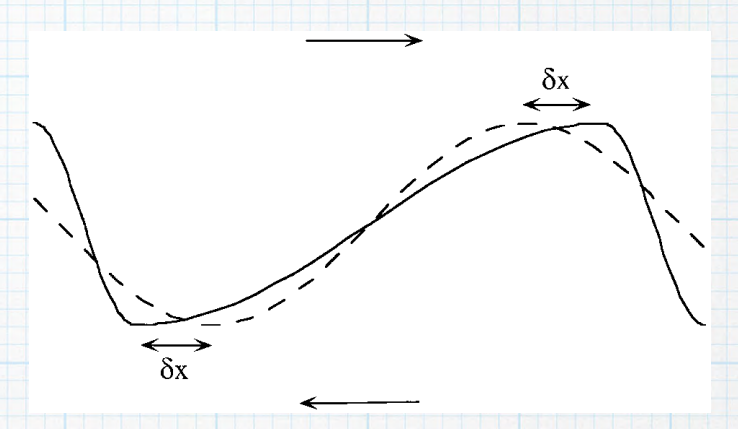
oriented lamellar in flow direction



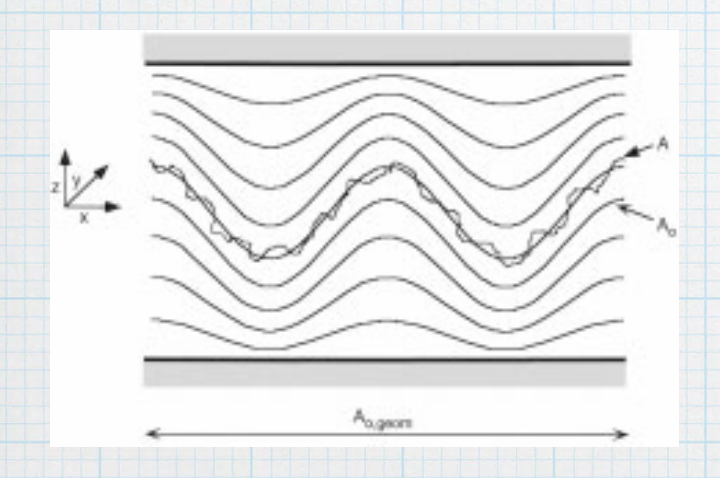
an onion formation mechanism: buckling



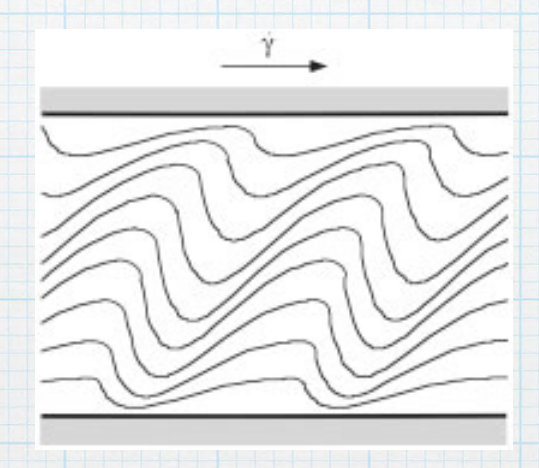
planar lamellar subject to shear



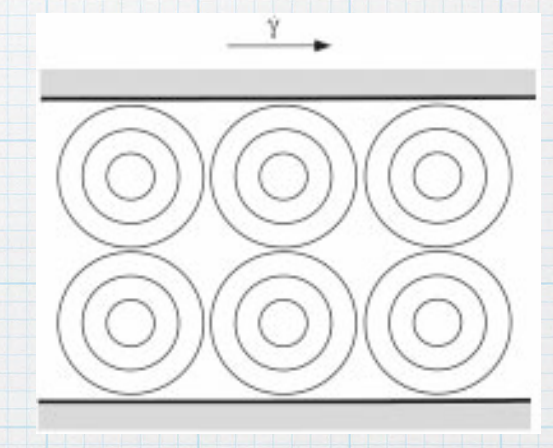
undulation fluctuation perturbed under shear flow generates an effective force to reduce an excess area



undulation instability



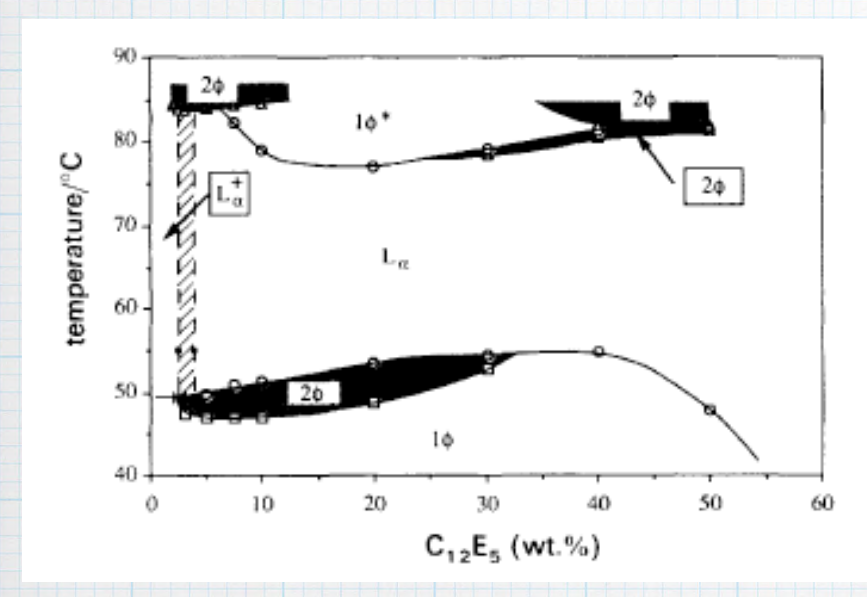
deformation of buckling



onion formation

charge effects in a surfactant membrane

water / $C_{12}E_5$ / SDS [SDS]/[$C_{12}E_5$] = 0.005

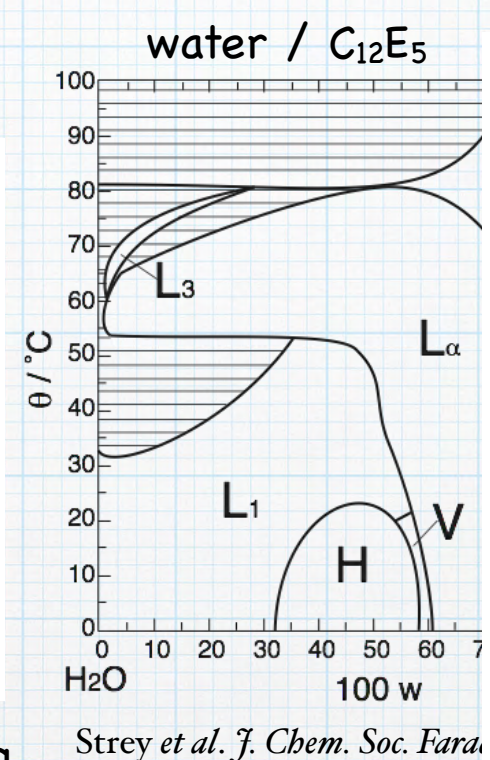


 L_{α} : birefringence only in streaming L_{α} : static birefringence

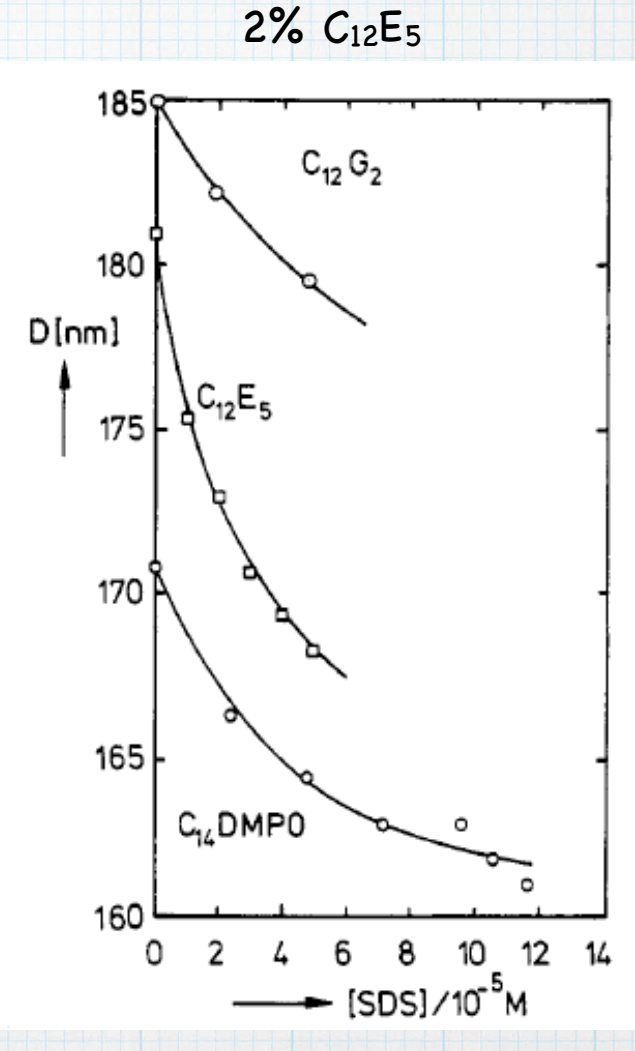
Douglas and Kaler J. Chem. Soc. Faraday Trans. 90, 471 (1994).

static birefringence multi lamellar structure (onion)

shear-induced onion formation



Strey et al. J. Chem. Soc. Fara 86, 2253 (1990).



Increasing charge density decreases d-spacing: lamellar peak appear in higher q with increasing charge

Schomacker and Strey J. Phys. Chem. 98, 3908 (1994).

Motivations

In order to clarify the mechanism of the onion formation, the buckling mechanism is verified by using neutron scattering techniques;

1. A mass fraction of 10% of $C_{12}E_5$ in water was selected as a model system for weak inter-lamellar interactions

the interaction is controlled by adding either anionic surfactant SDS, or antagonistic salt, RbBPh₄.

2. The bending rigidity of surfactant bilayers, κ , and the compressibility modulus, B, which are key parameters to express the critical shear rate or buckling wavelength, are estimated.

normal SANS and NSE with changing charge density in $C_{12}E_5$ bilayer by adding charged agent

3. MLV formation process at weak inter-lamellar interactions are compared with that at strong inter-lamellar interactions

rheology measurement together with rheo-SANS

1. structure change by adding charged agent

sample: lamellar phase of

nonionic surfactant C12E5 / D2O

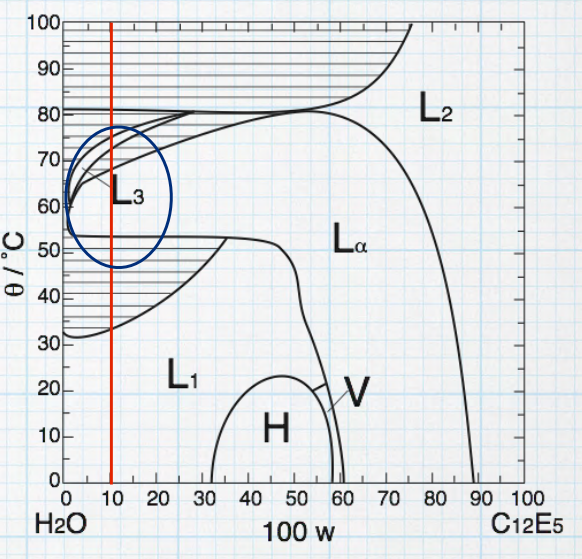
charged agent: anionic surfactant SDS

antagonistic salt RbBPh4

@ total surfactant concentration of 10 wt%

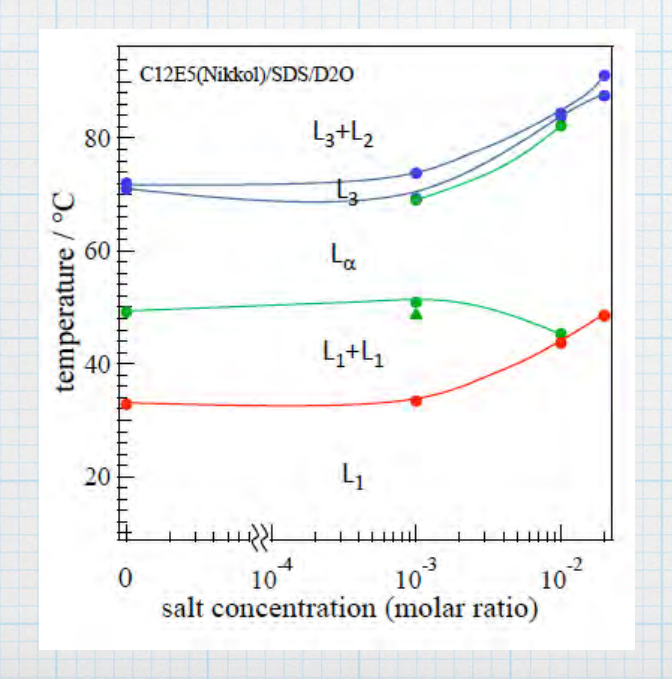
c.f. Gentile result for 40 wt%

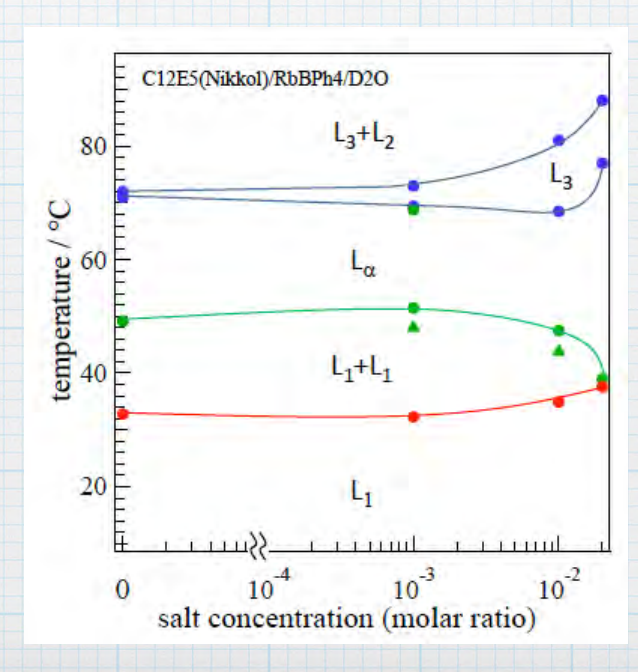
Gentile et al. Langmuir 27, 2088 (2011).



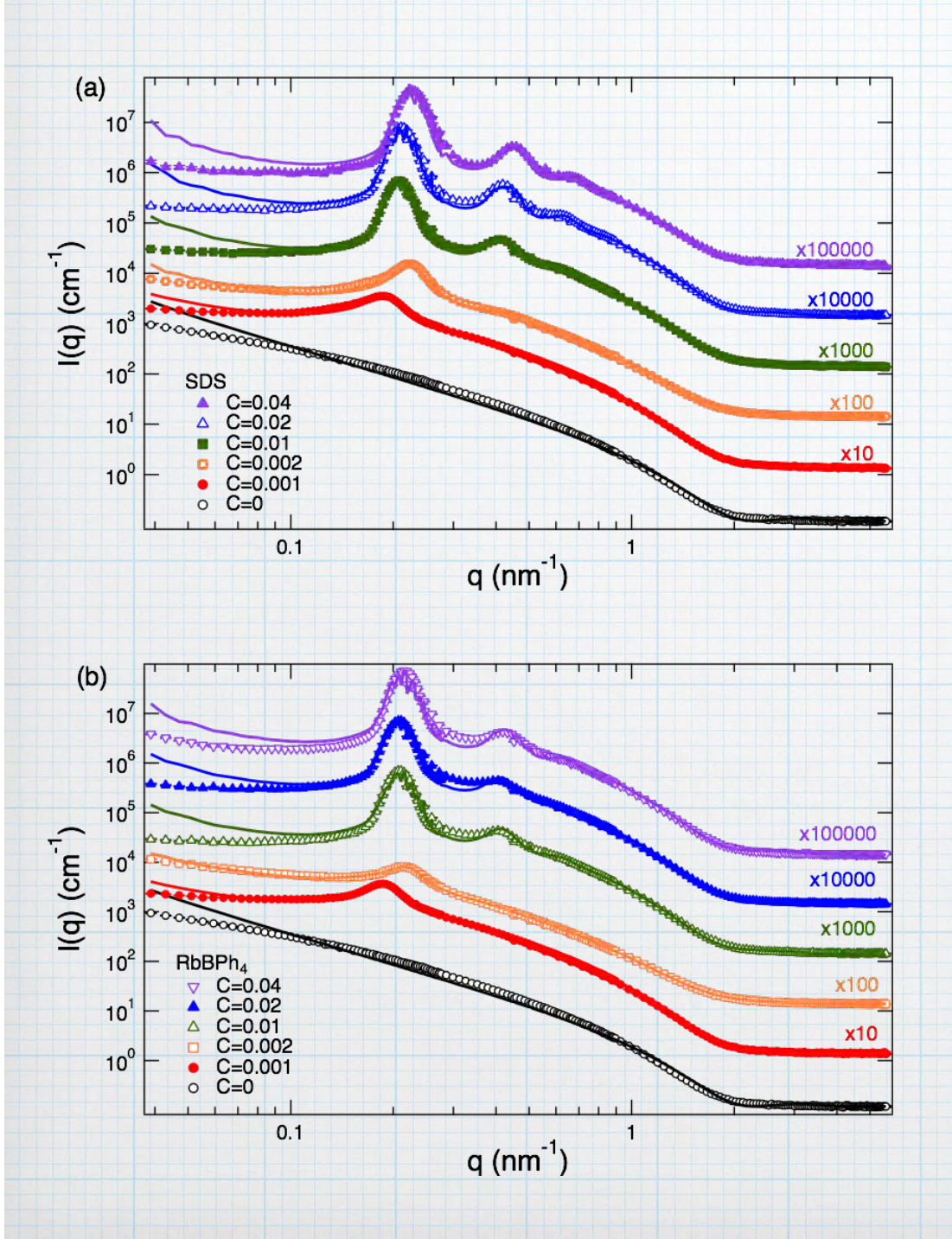
Strey et al. J. Chem. Soc. Faraday Trans. **86**, 2253 (1990).

experiment: on CG2 general purpose SANS at ORNL & NG7 30m SANS at NIST





1. structure change by adding charged agent



SANS patterns observed when increasing the amount of (a) SDS and (b) RbBPh₄ in C₁₂E₅ bilayers in D₂O at T=58°C.

Classification

Physics Abstracts
61.10D — 61.30E — 82.70

Modelling X-ray or neutron scattering spectra of lyotropic lamellar phases: interplay between form and structure factors

F. Nallet, R. Laversanne and D. Roux

Centre de recherche Paul-Pascal, CNRS, avenue du Docteur-Schweitzer, F-33600 Pessac, France

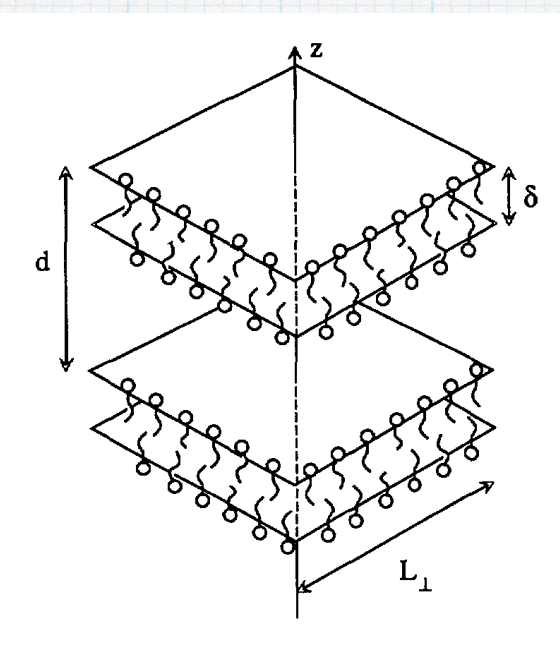


Fig. 2. — Geometrical model of a lyotropic lamellar L_{α} phase; the planar surfactant bilayer has a thickness δ ; the bilayers are stacked along the direction z with a period d.

Geometrical model

The intensity I_{id} of a radiation scattered at a wave vector \mathbf{q} by an irradiated volume V of a sample characterized by a scattering length density $\rho(\mathbf{x})$ is classically given by:

$$I_{id}(\mathbf{q}) = \left\langle \left| \int_{V} \rho(\mathbf{x}) e^{i\mathbf{q} \cdot \mathbf{x}} d^{3}\mathbf{x} \right|^{2} \right\rangle$$
 (1)

The scattering length density is defined by:

$$\rho(\mathbf{x}) = \sum_{0}^{N-1} \rho_0(z - nd), \quad |\mathbf{x}_\perp| < L_\perp$$

$$\rho(\mathbf{x}) = 0, \quad \text{otherwise}$$
(2)

P(q) is the form factor of the bilayer:

$$P(q) = \left| \int_0^\delta \rho_0(z) \, e^{iqz} \, \mathrm{d}z \right|^2 \tag{3}$$

Thermodynamical model

Caillé chooses a scattering length density of the following form:

$$\rho(\mathbf{x}) \propto \sum_{n} \delta \left\{ z - nd + u_n(\mathbf{x}_{\perp}) \right\}$$
 (4)

where $u_n(\mathbf{x}_{\perp})$, displacement along z of the n-th layer at the transverse position \mathbf{x}_{\perp} , has Gaussian fluctuations according to the harmonic elastic theory of smectic A phases [19]. The

Combining geometry with thermodynamics

Assuming that the n-th layer may fluctuate about its equilibrium position n. d by an amount u_n independent of the transverse coordinates.

$$\left\langle (u_n - u_0)^2 \right\rangle = \frac{\eta n^2 d^2}{8}, n \text{ small}$$

$$\left\langle (u_n - u_0)^2 \right\rangle = \frac{\eta}{2 \pi^2} \left[\ln (\pi n) + \gamma \right] d^2, \quad n \gg 1$$
(5)

with γ Euler's constant and η defined in terms of the elastic constants of the smectic phase \bar{B} and K by [15]:

$$\eta = \frac{q_0^2 k_{\rm B} T}{8 \pi \sqrt{K\bar{B}}}.$$
 (6)

With this amendment to the geometrical model, the scattering length density $\rho(x)$ becomes:

$$\rho(\mathbf{x}) = \sum_{0}^{N-1} \rho_0(z - nd + u_n), \quad |\mathbf{x}_\perp| < L_\perp$$

$$\rho(\mathbf{x}) = 0, \quad \text{otherwise}.$$
(7)

Substituting equation (7) into equation (1) leads to the following form for the intensity scattered by one isolated, finite-size crystal:

$$I_{id}(\mathbf{q}) = N \cdot P_{\perp}(\mathbf{q}_{\perp}) \cdot P(q_z) \cdot S(q_z)$$
 (8)

where P is the form factor of the bilayer, equation (3), S is the normalized structure factor of the stack:

$$S(q_z) = 1 + 2 \sum_{1}^{N-1} \left(1 - \frac{n}{N} \right) \cos(nq_z d) e^{-\frac{q_z^2}{2} \langle (u_n - u_0)^2 \rangle}$$
 (9)

and $P_{\perp}(\mathbf{q}_{\perp})$ accounts for the finite transverse size of the bilayers. Its exact expression depends on the shape of the plaquettes, with the following general properties: P_{\perp} is sharply peaked at $\mathbf{q}_{\perp} = \mathbf{0}$, with $P_{\perp}(\mathbf{0}) = L_{\perp}^4$; its width is of the order $2\pi/L_{\perp}$. It should be noted that our expression for the structure factor, equation (9), differs from those that result from « stacking disorder » of the first or second kind [6] (or, equivalently, for « perturbed regular lattices » or « paracrystalline lattices » [7]).

Thus, the experimentally-recorded intensity scattered by an irradiated volume V containing $V/N dL_{\perp}^2$ finite-size crystals randomly oriented is finally given by:

$$I_{\exp}(q) = 2 \pi \frac{V P(q) \tilde{S}(q)}{d^2}$$
(17)

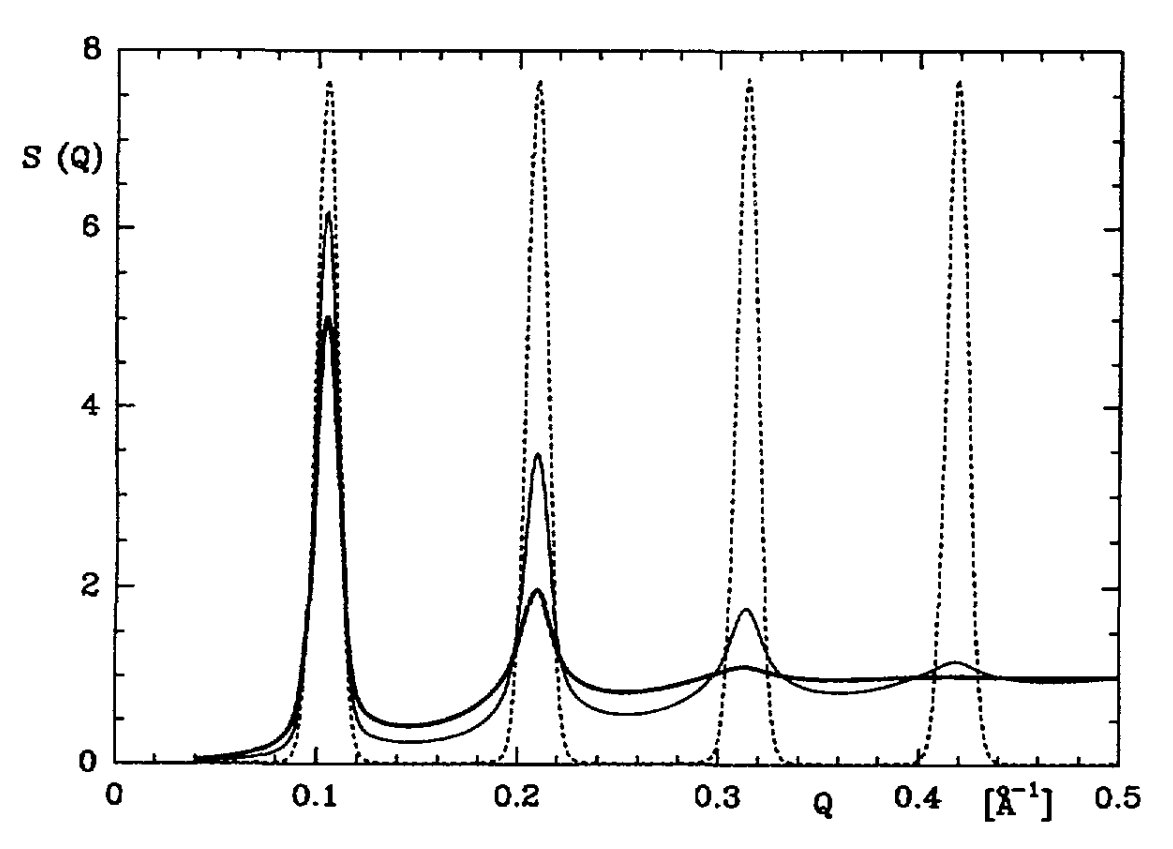
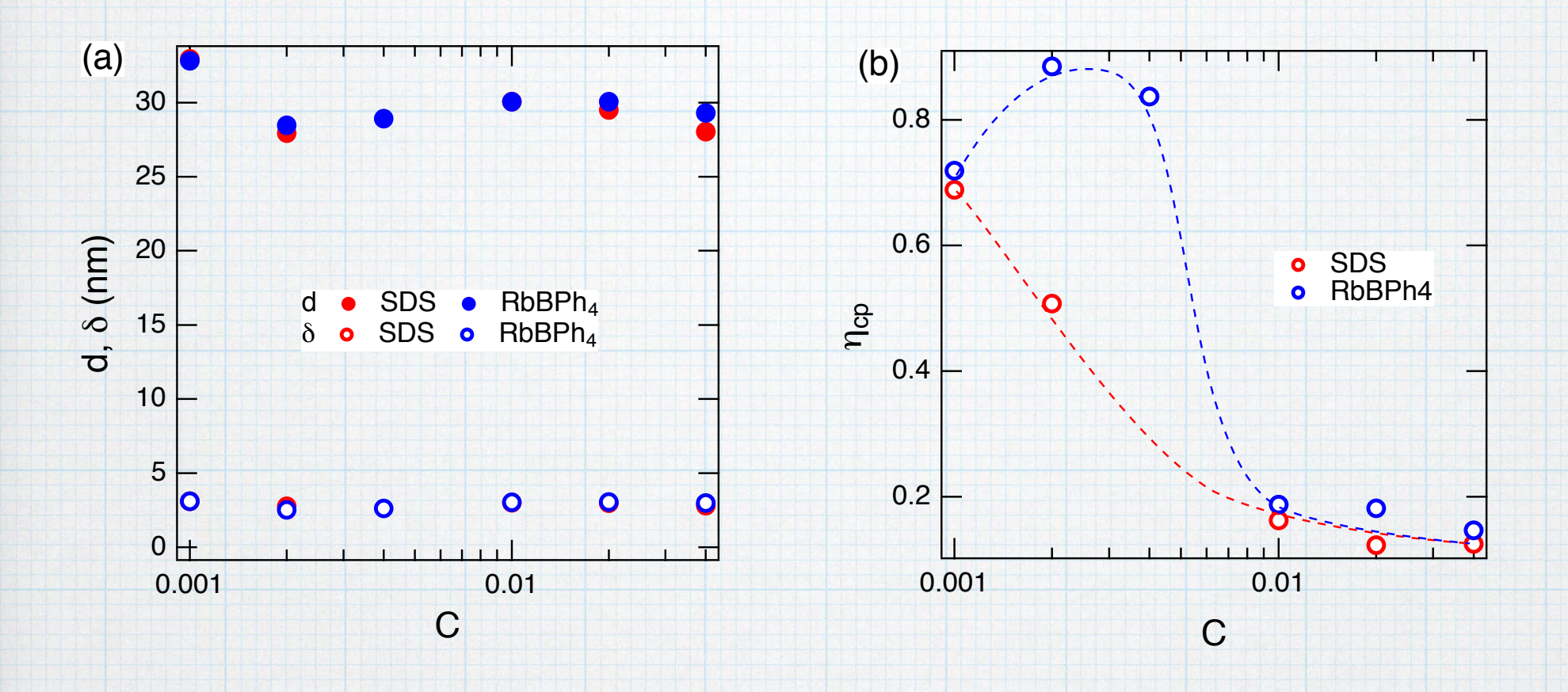


Fig. 6. — Structure factor of a d=60 Å lamellar phase with some layer displacement fluctuations; dotted curve: $\eta=0$; continuous curve: $\eta=0.1$; heavy line: $\eta=0.2$; the latter values of η are typical for lamellar phases stabilized with either weakly screened electrostatic interactions or undulation interactions [22]; the number of correlated layers in the stack is N=60 and a finite resolution $\Delta q=5.2\times 10^{-3} \, {\rm Å}^{-1}$ has been taken into account; note how quickly the function reaches its asymptotic value 1 when $\eta\neq 0$.

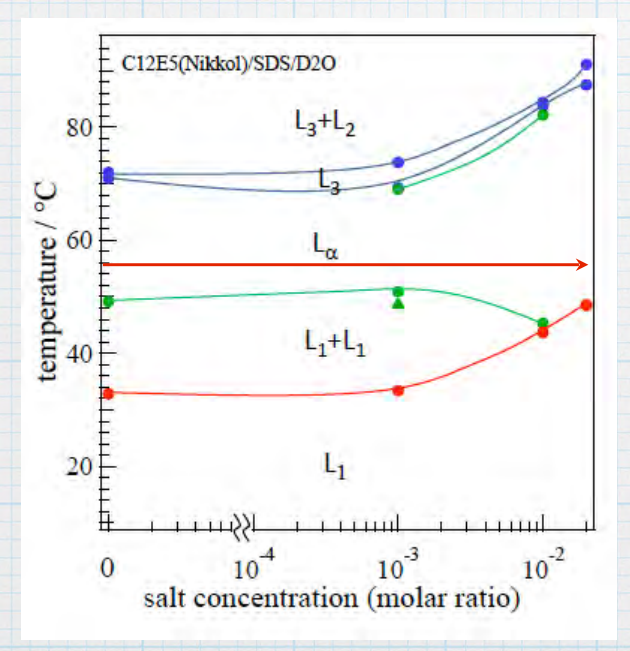


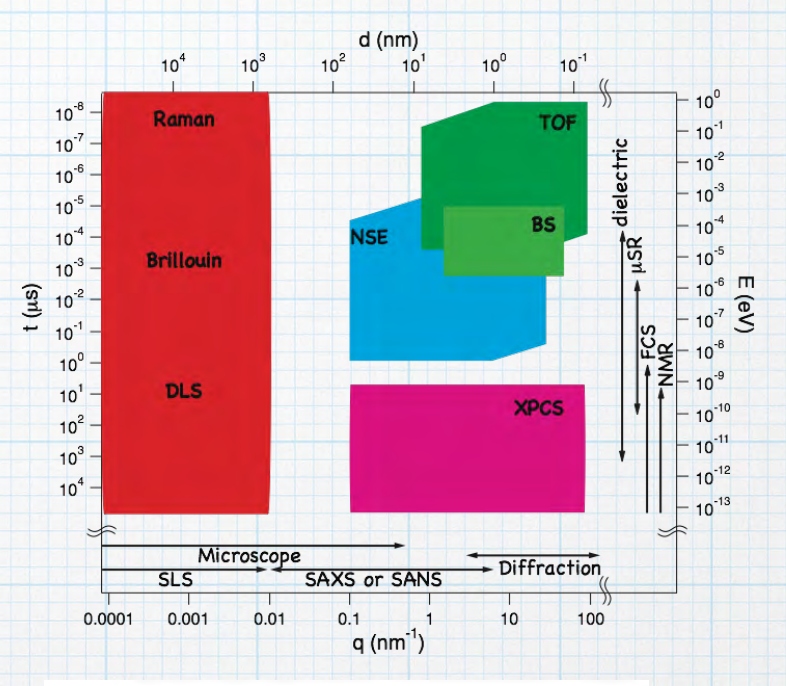
(a)Mean repeat distance d slightly decreases at low charge conditions while overall values may be almost constant around 30 nm. The bilayer thickness δ is al- most constant at 3.0 nm for both charge cases. (b)Extracted Caill'e parameter shows different behavior at low charge concentration cases between anionic surfactant and antagonistic salt.

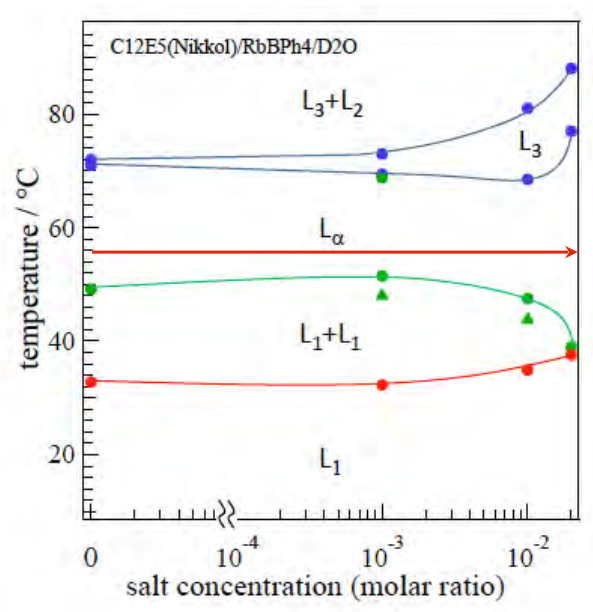
2. charge density dependence of membrane elasticity

experiment: on NGA-NSE at NIST

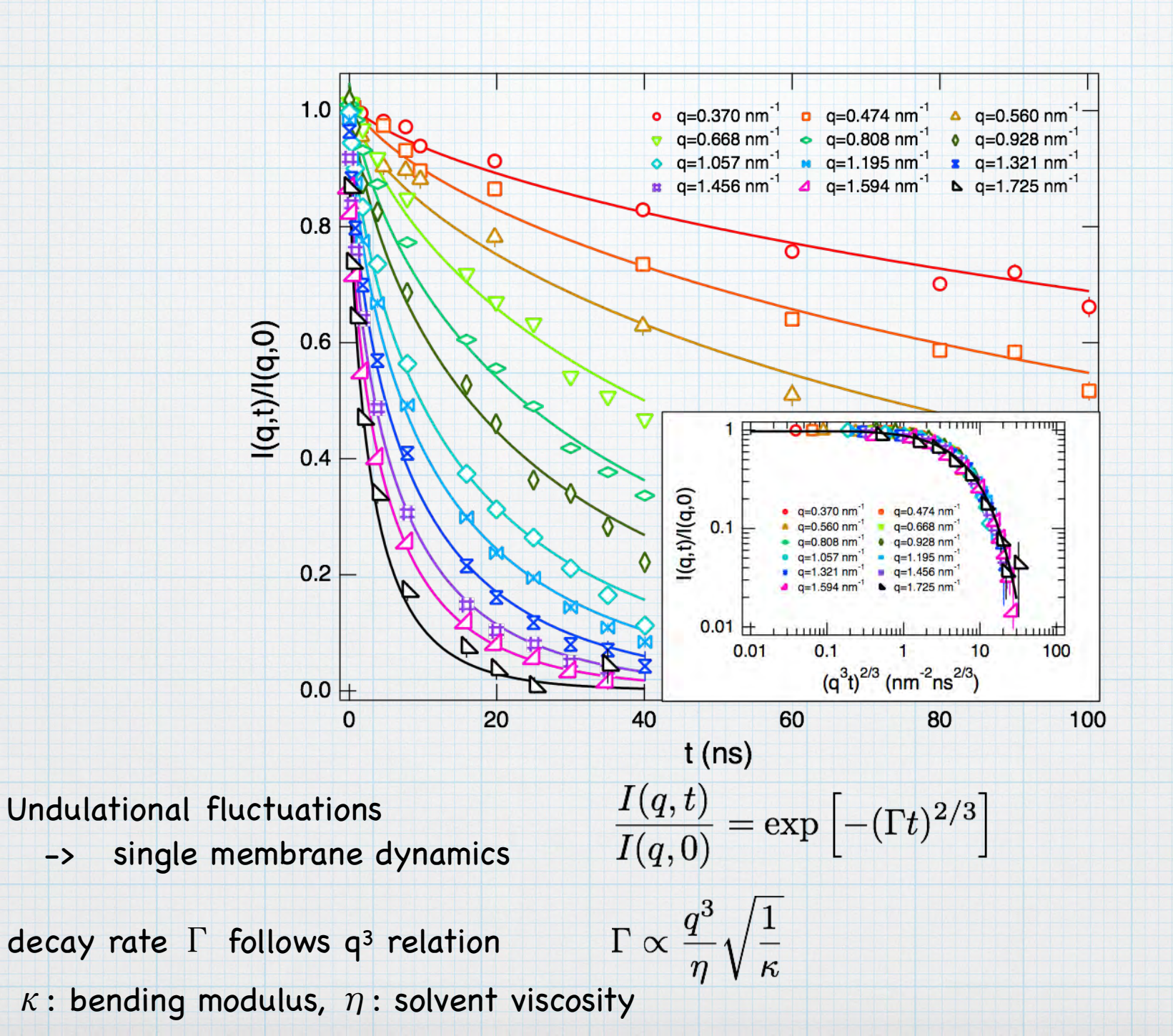








2. charge density dependence of membrane elasticity



Single membrane fluctuation

Zilman and Granek

A lateral length *L* along the membrane flat surface is perturbed in some way, because they are 2D connected object.

$$h \simeq (k_B T/\kappa)^{1/2} L^{\zeta}$$
 roughness exponent: $\zeta = 1$ (2D object)
= 3/2 (1D object)
 $L \simeq (\kappa/k_B T)^{1/2\zeta} Q^{-1/\zeta}$

The Stokes-Einstein diffusion coefficient is,

$$D(Q) \simeq (k_B T/\eta L) \simeq (k_B T/\eta)(k_B T/\kappa)^{1/2\zeta} Q^{1/\zeta}$$

The relaxation rate is,

$$\Gamma(Q) \simeq D(Q) Q^2 \simeq (k_B T/\eta) (k_B T/\kappa)^{1/2\zeta} Q^{2+(1/\zeta)}$$

Thus they obtained the stretched exponential form of the relaxation function as,

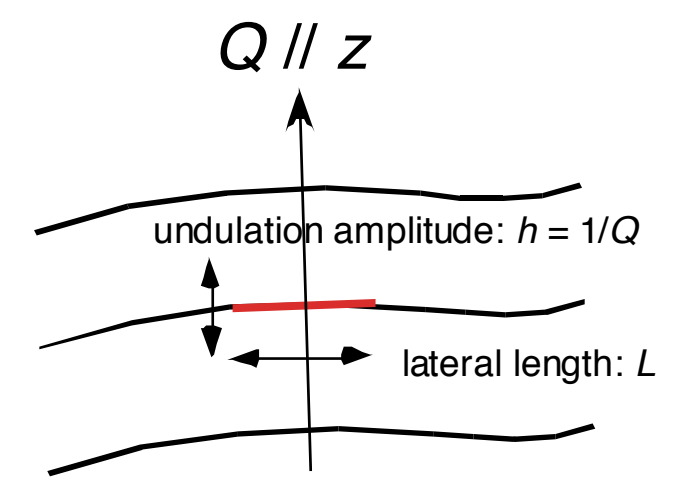
$$I(Q, t) = \exp[-(\Gamma(Q)t)^{\beta}]$$

where

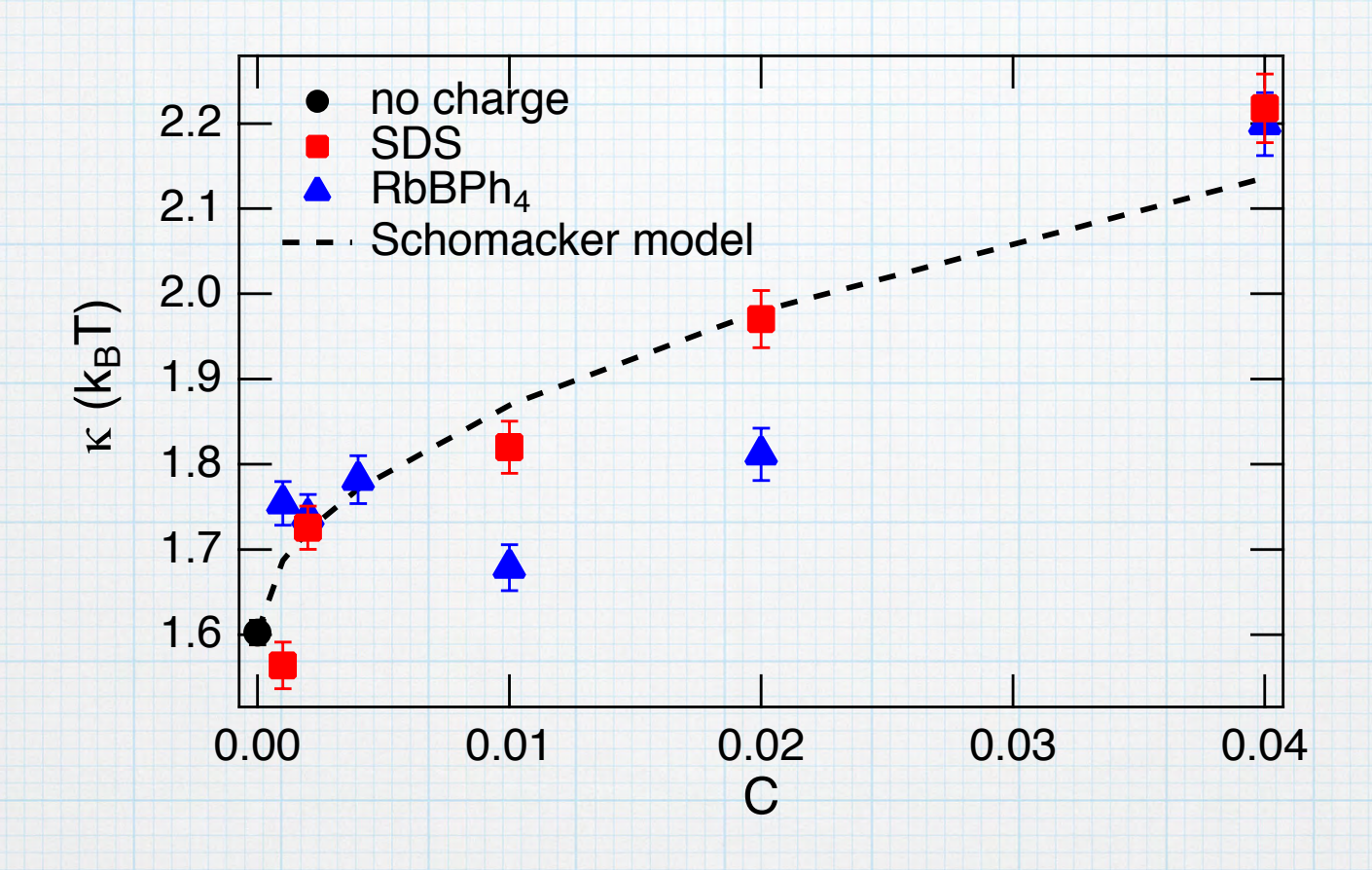
$$\Gamma(Q) = \gamma_{\alpha} \gamma_{\kappa} (k_{B}T)^{1/\beta} \kappa^{1-(1/\beta)} \eta^{-1} Q^{2/\beta}$$

with

$$\beta$$
 = 2 / (2+1/ ζ) = 2/3 (2D object) γ_{α} = 0.024 (2D object) = 3/4 (1D object) = 0.0056 (1D object) γ_{κ} = 1 - 3 ln(ξ / $I(t)$) $k_{B}T$ / (4 $\pi\kappa$)



2. charge density dependence of membrane elasticity



 Increasing charge density of a bilayer slightly increases bending modulus, and they follow the theoretical prediction proposed by Schomächer and Strey.

$$\kappa_c=3k_BT/4\pi\kappa_D^3l_Bl_{GC}^2$$
 $\kappa_D^{-1}=\sqrt{\epsilon_r\epsilon_0k_BT/2ne^2}$: Debye length $l_B=e^2/4\pi\epsilon_r\epsilon_0k_BT$: Bjerrum length $l_{GC}=e/2\pi l_B\sigma$:Gouy-Chapman length

charge effects on the steady state structure and dynamics

The dilution law (d= δ / ϕ) can be modified due to the membrane undulation

$$d = \delta(1 + \frac{\Delta A}{A})/\phi$$

A: area of the undulating bilayer projected on the plane normal $\Delta A+A$: average of the true area of the bilayer

de Vries proposed to compare relative change in the dilution relation and area change as

$$\left(\frac{d\phi}{\delta}\right)_2 - \left(\frac{d\phi}{\delta}\right)_1 = \left(\frac{\Delta A}{A}\right)_2 - \left(\frac{\Delta A}{A}\right)_1$$

$$\left(\frac{\Delta A}{A}\right)_n = \frac{1}{4\pi\kappa_n} \int_0^{x_m} \frac{dx}{x} \left(1 + \frac{d_{w,n}}{\pi l_B \kappa_n} \frac{f_e(x,\Lambda)}{x^4}\right)^{-1/2}$$

$$\times \left(1 + \frac{d_{w,n}}{\pi l_B \kappa_n} \frac{f_0(x,\Lambda)}{x^4}\right)^{-1/2}$$

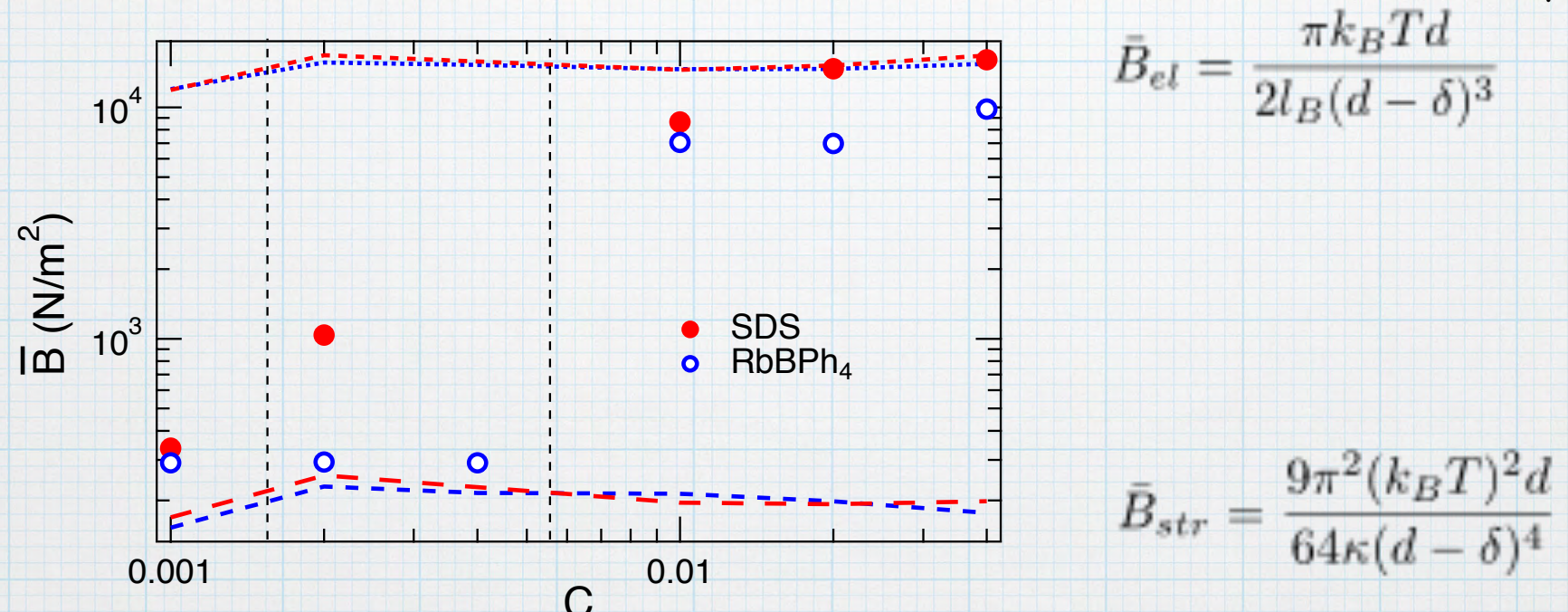
the reduction of undulation fluctuations due to the increase in the bending rigidity of membranes cannot explain the change of the value of d

charge effects on the layer compressibility modulus

The layer compressibility modulus B was calculated from κ and $\eta_{\rm \, cp}$ in

$$\eta_{cp} = \frac{q_p^2 k_B T}{8\pi \sqrt{\kappa \bar{B}/\delta}}$$

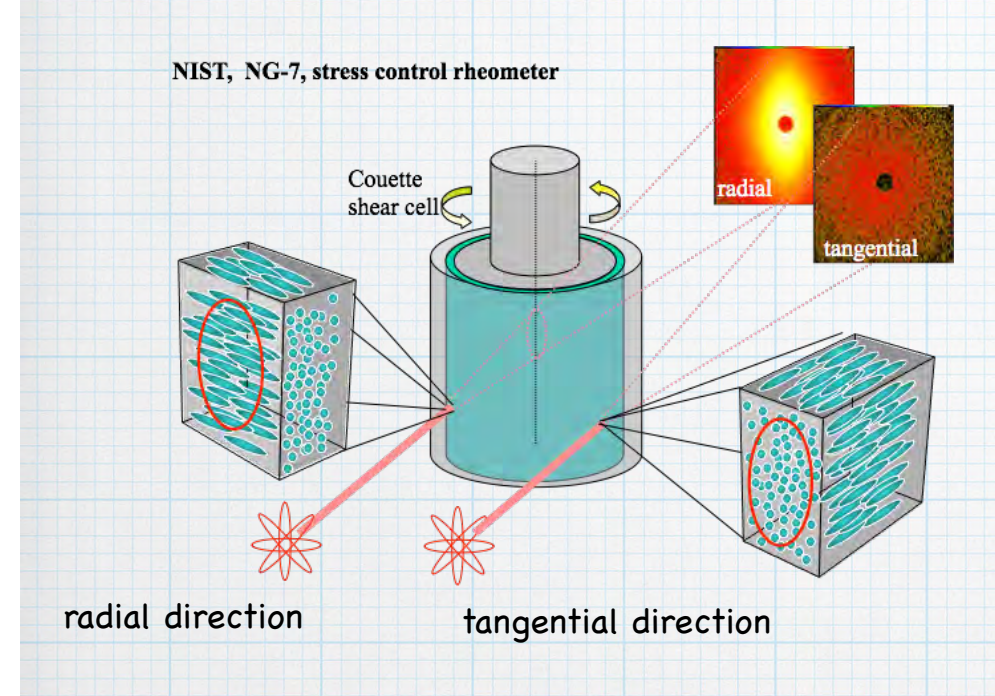
Weakly screened electrostatic repulsion

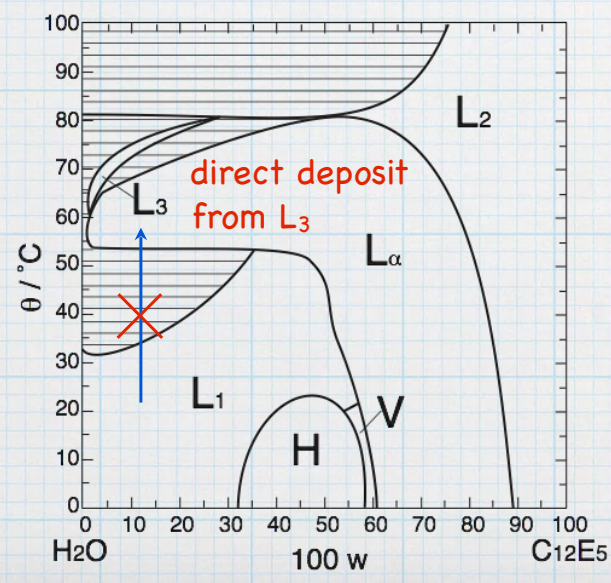


Steric repulsion due to thermal undulations

3. shear-induced MLV formation

experiment: rheology measurement & NGB 10m SANS at NIST





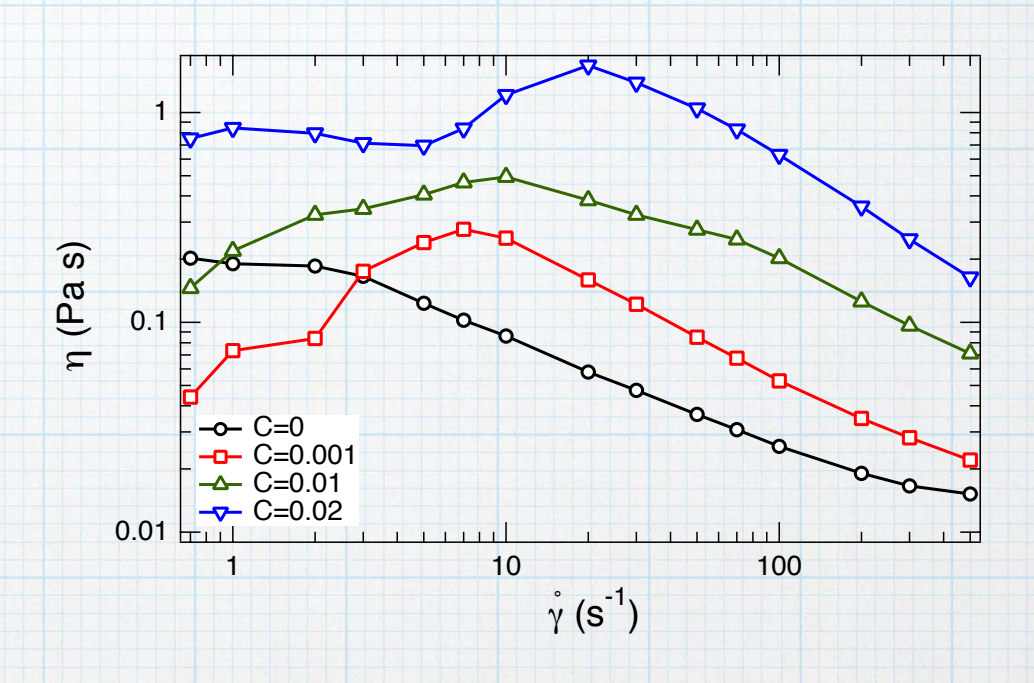
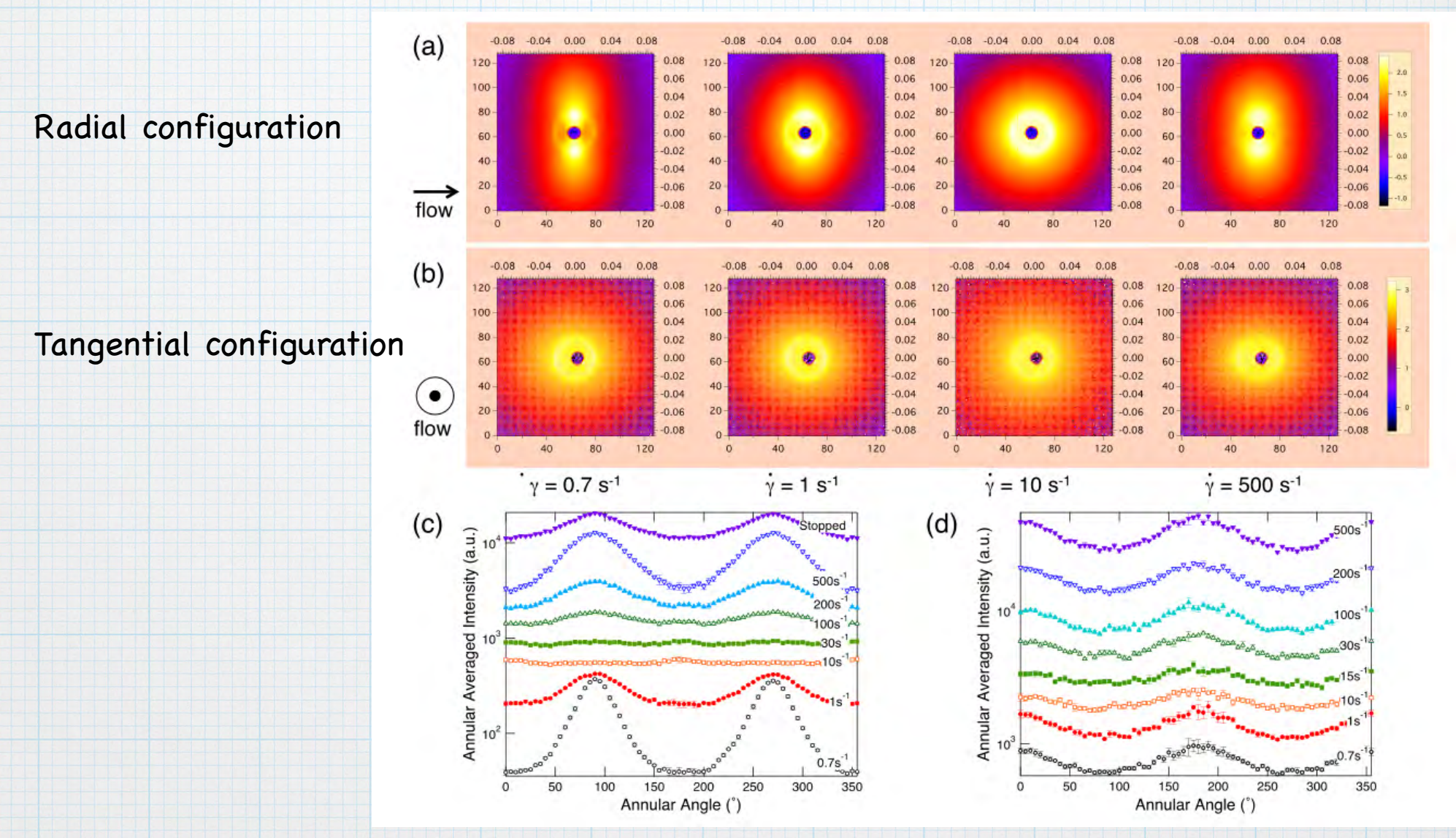


FIG. 8. (Color online) Apparent viscosity in $C_{12}E_5/SDS/D_2O$ systems under shear at $C=0,\ 0.001,\ 0.01$ and 0.02. Shear thickening is observed around $\dot{\gamma}_c=10\ s^{-1}$. The pure sample shows a slight shoulder around $\dot{\gamma}_c=3\ s^{-1}$, which can be a similar trend to the shear thickening seen in the charged systems.

3. shear-induced MLV formation

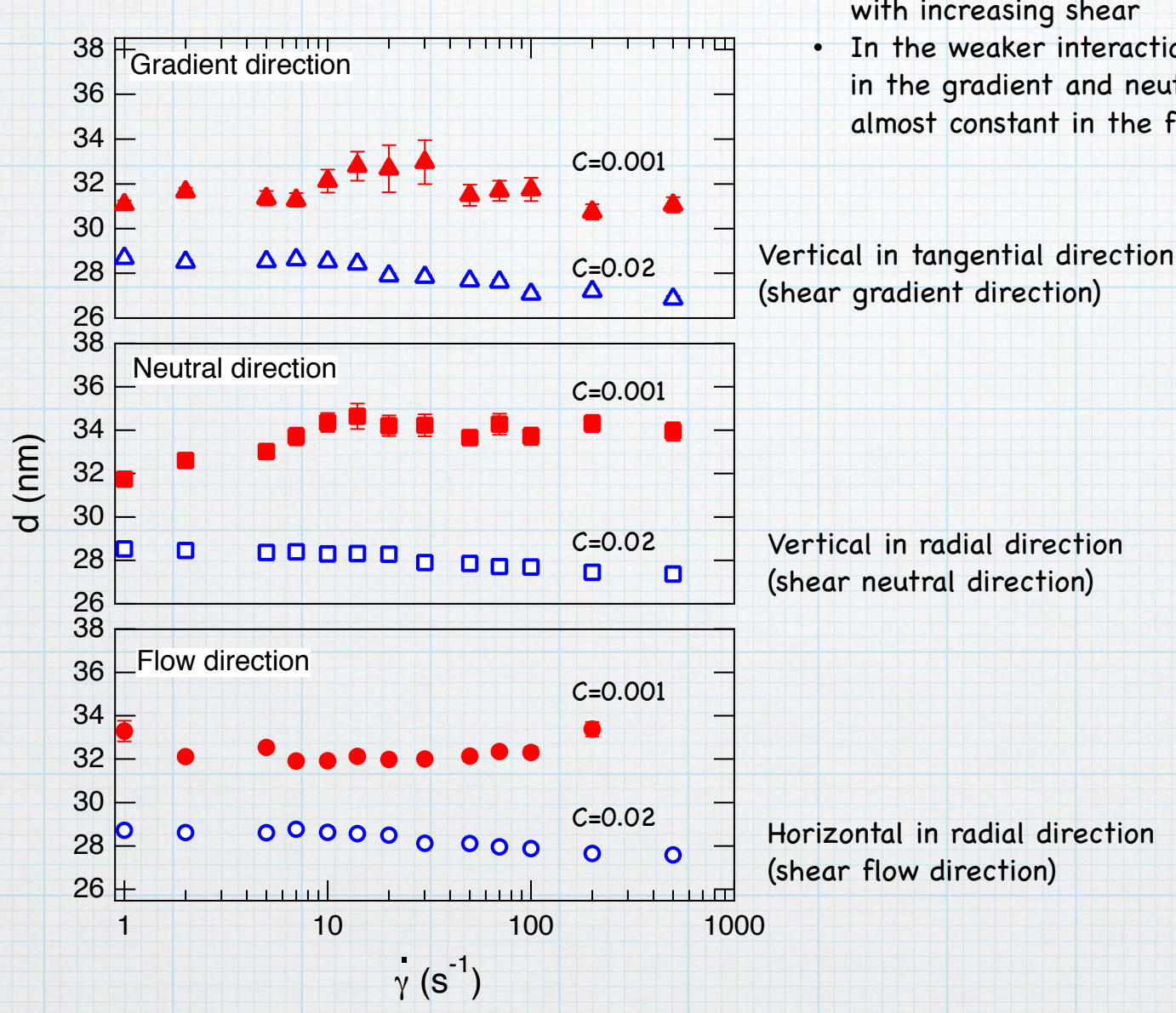
 $C_{12}E_5 / D_2O / RbBPh_4$, C=0.001



Annular average of the 2D SANS pattern at q=0.2 nm⁻¹ for (c) radial and (d) tangential configuration

3. shear-induced MLV formation

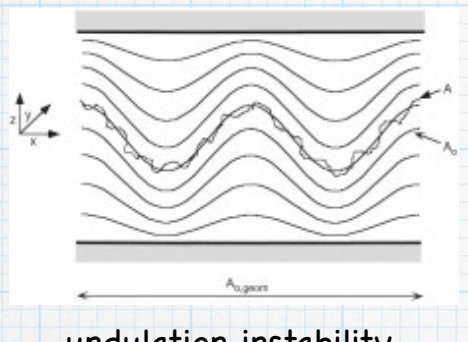
C₁₂E₅ /D₂O / SDS, C=0.001 and 0.02

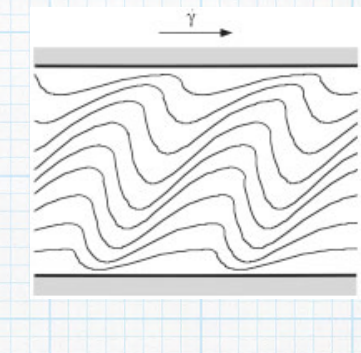


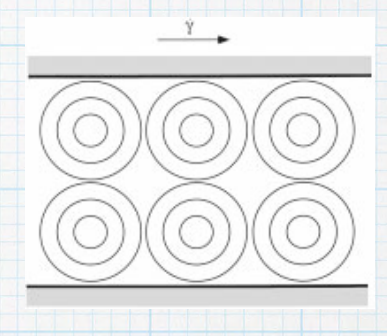
- The larger interlayer interaction case (C=0.02), d stays almost constant below the critical shear rate and decreases with increasing shear
- In the weaker interaction case (C=0.001), d increases both in the gradient and neutral directions at low shear, while almost constant in the flow direction.

Summary

Stronger interaction case





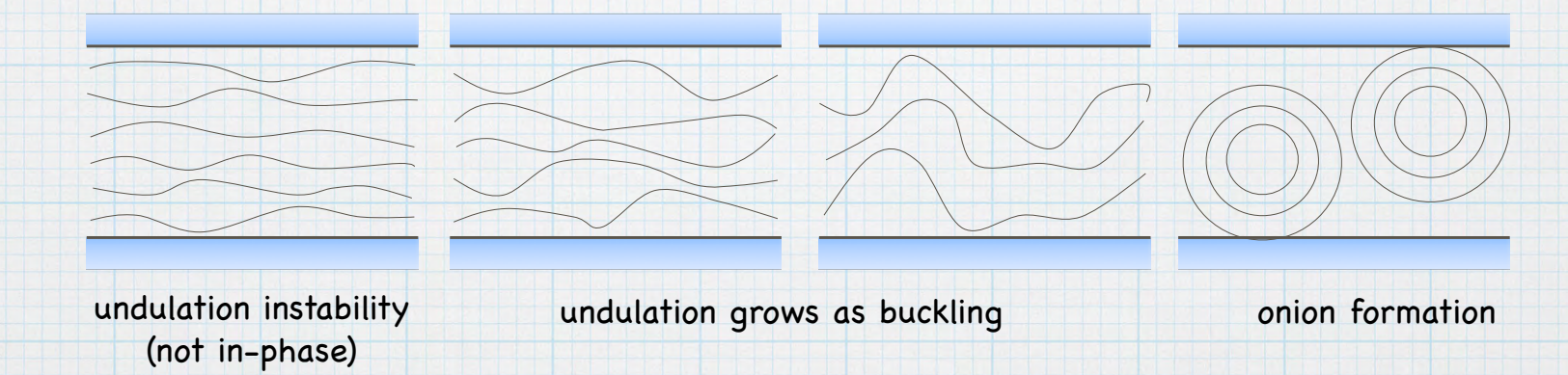


undulation instability

deformation of buckling

onion formation

Weaker interaction case



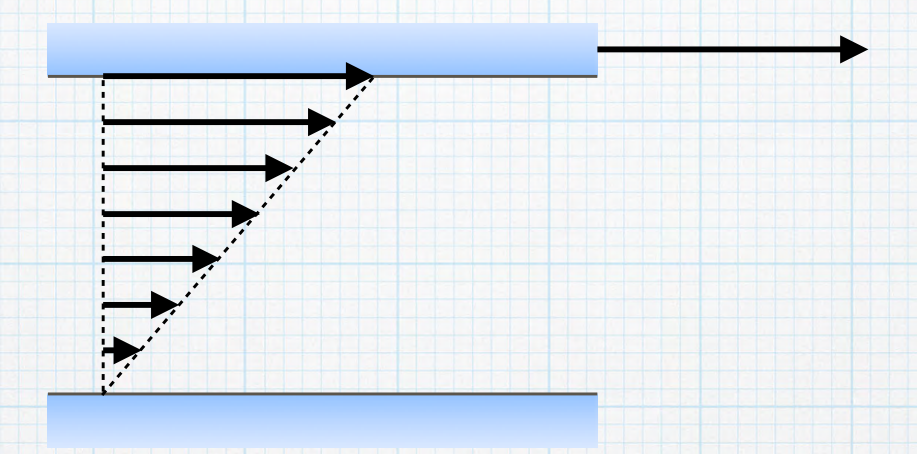
The increase of d is induced by the increased undulation due to the flow, which corresponds to the increase of the buckling instability.

Difference in structural changes of surfactant aggregates near solid surface under shear flow versus those in the bulk

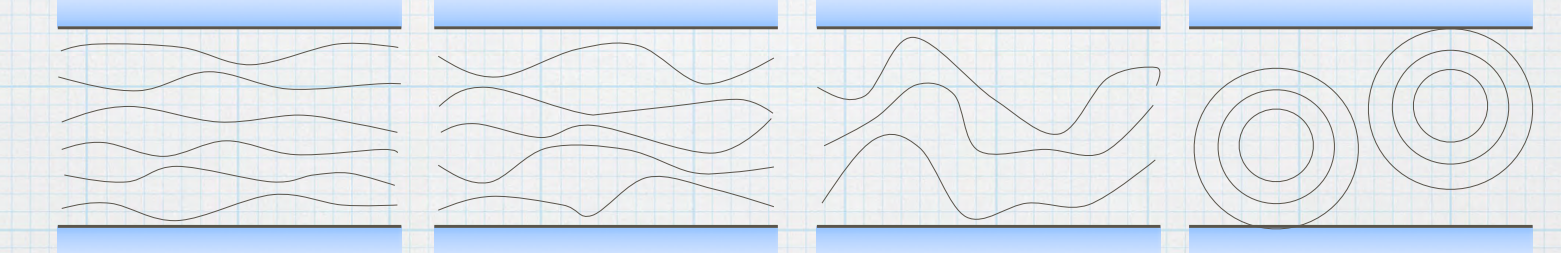
F. Nemoto (National Defense Academy)
F. Takabatake, N. L. Yamada, H. Seto (KEK)
S. Takata (JAEA)

Rheology

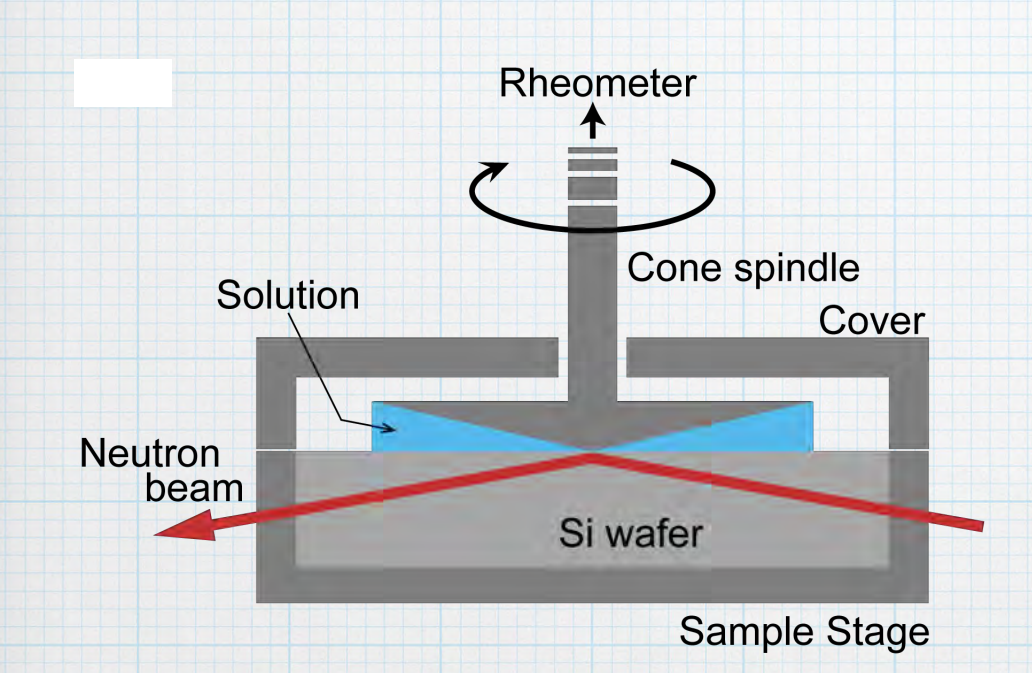
Non-slip condition at the interface is assumed



Surfactant membranes may slip on the solid substrate



Neutron Reflectometer SOFIA(@J-PARC, BL16)



injected neutron beam: -0.9° (penetration depth was about 30 μ m) footprint: 30mm×40mm

- Cone-plate type rotational viscometer (Brookfield RST-CC + custom stage) cone spindle
 - diameter:50mm
 - cone angle: 1°
- surfactant solution (C₁₂E₅/SDS)/D₂O (10wt%)

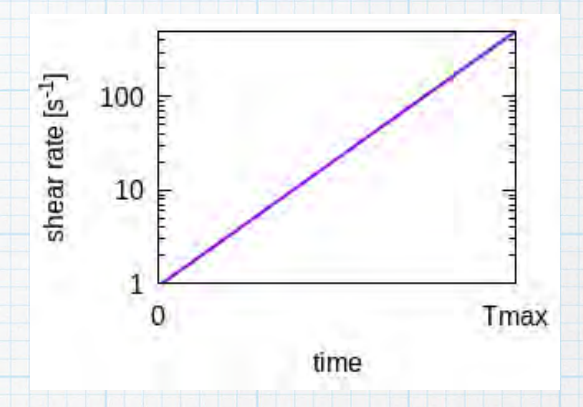
 $C = [SDS]/[C_{12}E_5]$ (molar ratio)

- Si wafer
 hydrophilic treatment by ozone/UV
 irradiation for 20 min.
- Temperature: 58.1 ~ 58.8 ° C → lamellar structure

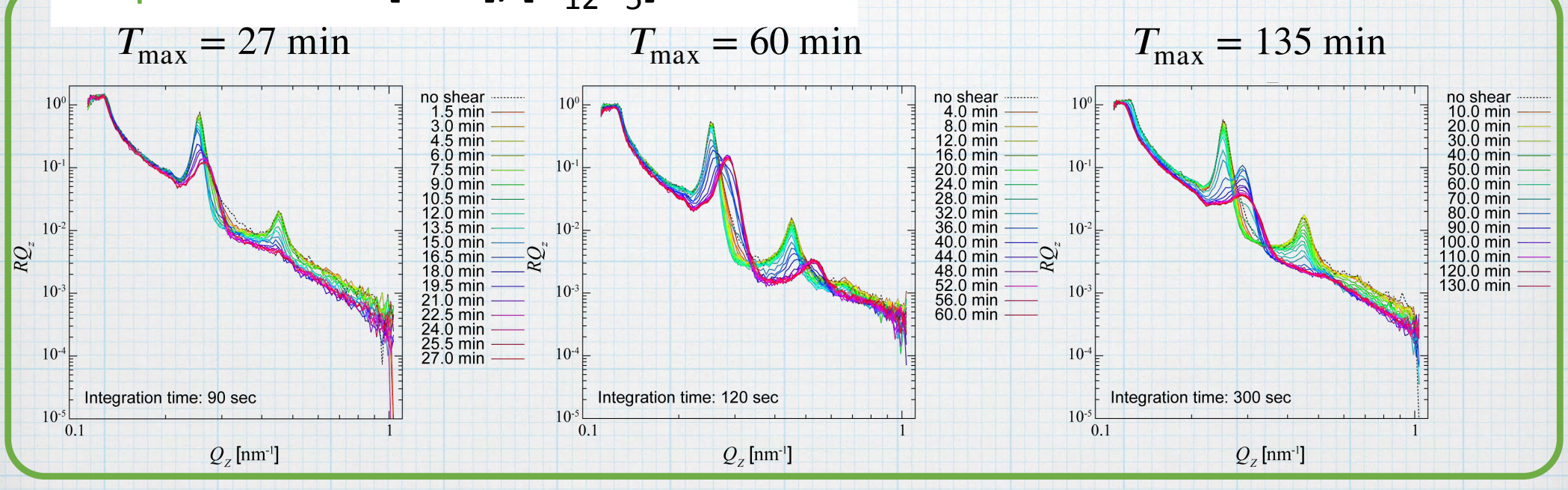
(Y. Kawabata et al., J. Chem. Phys. 147 (2017))

NR results

- The shear rate was increased from 1 to 500 s⁻¹ exponentially.
- The stacking structure was changed with increasing shear rate.
- The structural change depended on the increasing rate.







Shear-rate dependence by SANS

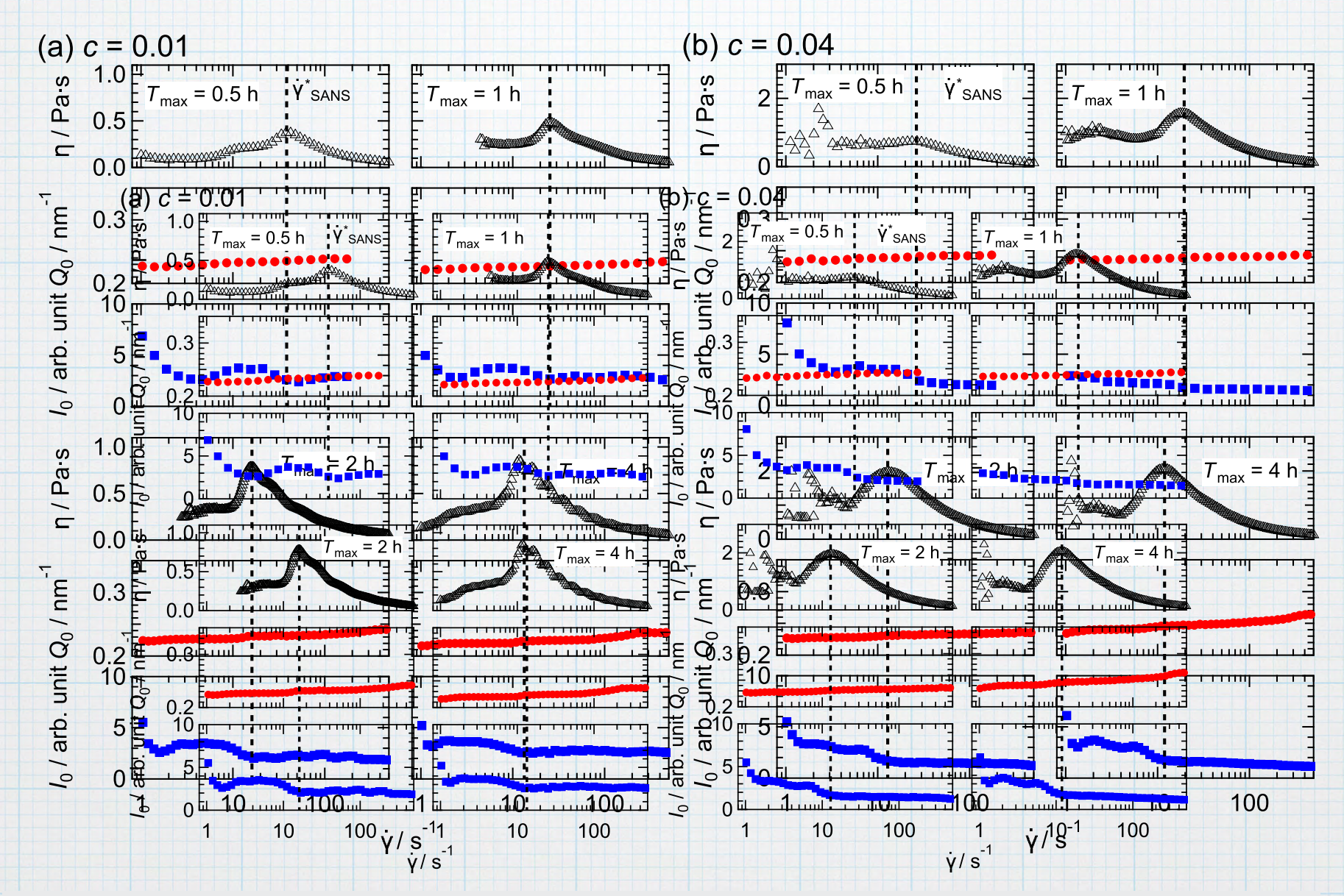


FIG. 3. Shear-rate-dependence of the viscosity η , the first Bragg peak position Q_0 , and the Bragg peak height I_0 for $T_{\text{max}} = 0.5$, 1, 2, and 4 h when (a) C = 0.01 and (b) C = 0.04 observed by SANS, respectively. The dashed vertical lines are the shear rate of the maximum viscosities, $\dot{\gamma}_{\text{SANS}}^*$. The error bar sizes are comparable to those of the data symbol size for the SANS data.

Shear-rate dependence by NR

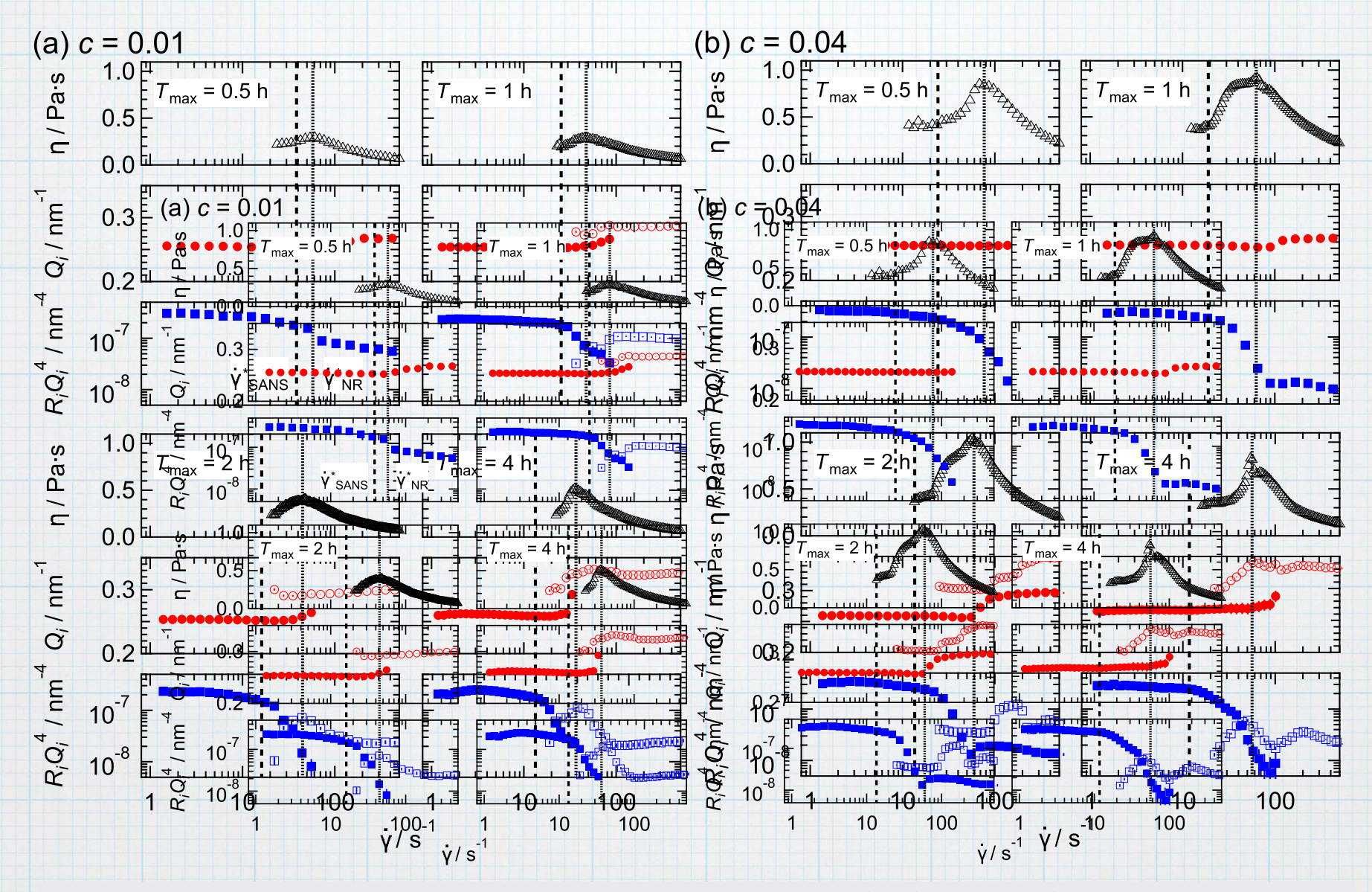


FIG. 6. Shear-rate-dependence of the viscosity η , the Bragg peak positions Q_i , peak height normalized by Q_i^4 , $R_iQ_i^4 = R(Q_z = Q_i)Q_i^4$ for $T_{\text{max}} = 0.5$, 1, 2, and 4 h when (a) C = 0.01 and (b) C = 0.04, where i = A1, B. Filled symbols indicate the peaks at Q_{A1} and open symbols indicate the peaks at Q_{B1} described in the main text. The dashed vertical lines represent the shear rate of the maximum viscosity observed using Rheo-SANS $\dot{\gamma}_{\text{SANS}}^*$, and the dotted vertical lines are those observed by Rheo-NR, $\dot{\gamma}_{\text{NR}}^*$, respectively. The error bar sizes are comparable to those of the data symbol size for the NR data.